Study of the shadow effect caused by a railway tunnel

Qiyun Jin, David Thompson

Institute of Sound and Vibration Research, University of Southampton, Southampton SO17 1BJ, UK

Q.Jin@soton.ac.uk

Abstract. When a train runs in a tunnel the largest vibration on the ground surface may not occur directly above the tunnel but at some lateral distance away from the tunnel alignment. This has been called the 'shadow effect'. The characteristics of this shadow effect can help in understanding the distribution of vibration on the ground surface. For the current study it is first shown, using an analytical ground model, that a shadow region may occur for a force at some depth in the ground even in the absence of a tunnel; the extent of this effect depends on the Poisson's ratio of the soil. To introduce the tunnel a 2.5D finite element/boundary element model has been used to represent the coupled tunnel-ground situation. When the tunnel is present the vibration caused by excitation at the tunnel base shares many of the features found in the absence of the tunnel. However, the existence of the tunnel structure also influences these features, especially at high frequencies. It is found that, rather than the tunnel structure shielding the vibration from reaching the ground surface, its dominant effect is to transmit vibration from the tunnel base to the crown at high frequencies. The dependence of these effects on various parameters is studied, in particular the tunnel diameter, wall thickness and depth.

1. Introduction

The prediction of vibration on the ground surface due to a train running in a tunnel is an important step in evaluating the ground-borne noise in buildings. The responses have been investigated by many researchers using various methods. A two-dimensional (2D) model, using a combination of the finite element and boundary element methods, was developed by Jones et al. to study the transmission properties of ground vibration caused by a train in a tunnel [1]. It was found in their study, by comparing an unlined tunnel with a lined one, that the tunnel lining affects the distribution of displacements on the ground surface. In both cases the peak responses occurred at some distance away from the tunnel centreline. The same phenomenon is also described in [2] as an area of vibration amplification caused by the existence of the tunnel structure.

In this paper, the phenomenon is described as a shadow effect, and its characteristics will be studied using both analytical and numerical models. It is shown that the phenomenon also occurs in the absence of a tunnel for a force at some depth in the ground. Due to the existence of the shadow area, it is difficult for empirical models to predict accurately the vibration of buildings located within the shadow zone. Besides, the shadow effect and the location of highest amplitude are the most important places for predictions to be accurate.

Train-induced ground vibration can be predicted using various models. Analytical models, such as PiP (Pipe-in-pipe) [3], are computationally fast. However, numerical models are more flexible and can

include more details. In [4], both the 2D and 3D FE-BE models of the tunnel and ground were proposed and compared. The 3D model can give an accurate prediction for the absolute vibration levels but at a high computational cost. As an alternative to the 3D model, for situations with a constant cross-section, a 2D FE/BE mesh can be used and the third direction can be calculated at a series of wavenumbers. The full three-dimensional field is reconstructed using an inverse Fourier transform. This wavenumber FE/BE approach, also known as a 2.5D approach, has been used in [5] and [6] for the efficient prediction of train-induced vibration from surface and tunnel railways. This approach is also used in this paper for the calculation of response on the ground surface to the excitation in the tunnel, using in-house software WANDS (Wave Number Domain Software) [7].

2. Model description

In order to predict the vibration transmitted from the dynamic forces acting on a tunnel to the ground surface, a numerical model is constructed based on the wavenumber finite / boundary element method [6]. The cross-section of the tunnel is modelled with finite elements whereas boundary elements are used for the ground including the free surface, as shown in figure 1. The geometry of the tunnel is modelled with 30 8-node solid elements. The inner and outer diameters of the tunnel are 3.81 m and 4.11 m respectively, giving a wall thickness of 0.15 m. The ground is represented by boundary elements, with 30 m on each side of the tunnel centreline with a node spacing of 0.25 m. The soil properties and tunnel materials are given in table 1. The soil represents London clay [8] with a shear wave speed of 220 m/s and a compressional wave speed of 1570 m/s, the latter corresponding to saturated ground.

The third direction, which is assumed to be invariant, is converted from the wavenumber domain. The total number of wavenumbers calculated is 2048, at a linear spacing of 0.006 rad/m.

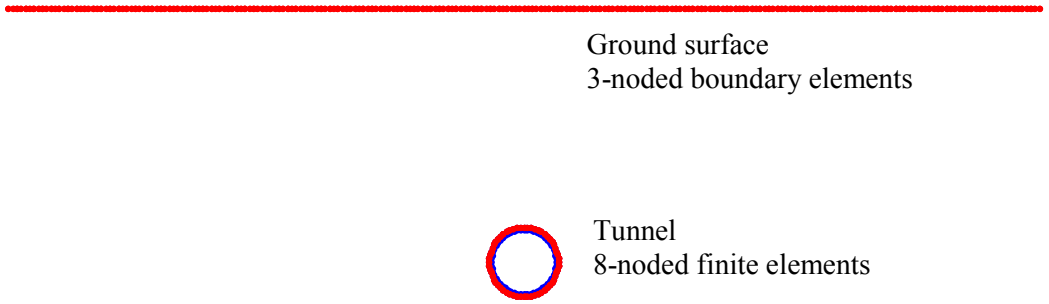

Figure 1. 2D FE / BE cross-section of tunnel-ground model.

Table 1. Soil properties and tunnel materials used in the model [8].

London clay	**S-wave speed**	**P-wave speed**	**Density**	**Loss factor**
	220 m/s	1570 m/s	1980 kg/m^3	0.078
Concrete tunnel	**Young's Modulus**	**Density**	**Poisson's ratio**	**Loss factor**
	50 GPa	2500 kg/m^3	0.3	0.03

3. Definition of shadow effect and corresponding parameters

Using the 2.5D FE / BE tunnel-ground model, the vertical displacements on the ground surface excited by a unit vertical force acting at the tunnel bottom are plotted in figure 2 for some example frequency bands. The depth from the ground surface to the tunnel centre is 15 m. The results have been converted from narrow frequency band to one-third octave bands with 3 frequencies per band.

Depending on the frequency, a region of high response can be found at some distances in figure 2. At 8 Hz, the maximum response occurs directly above the tunnel centreline. For the frequencies above 16 Hz, however, the region of maximum response occurs at some distance away from the centreline and the response above the tunnel is up to 10 dB lower. This is the so-called shadow effect in which the area above the tunnel appears to be in the 'shadow' of the tunnel. Figure 3 shows the 2D cross-section of the tunnel (in black dots) and the exaggerated deformation of the tunnel structure at 31.5 Hz (in red dots). This shows that the vibration at the crown of the tunnel is smaller than that at the bottom which may be linked to the smaller vibration above the tunnel in figure 2. It is the purpose of this paper to explore the reasons for this phenomenon in more detail.

Some parameters are used in the paper to describe the characteristics of the shadow effect. The frequency above which the shadow effect can be observed is called the cut-on frequency. For frequencies above the cut-on (e.g. 16, 31.5 and 63 Hz in figure 2), the maximum response is observed at some distance away from the tunnel centreline. The width of the shadow area is described by twice the distance from the position of maximum response to the tunnel centreline. A third parameter will also be used to define the magnitude of the shadow effect. This is the difference between the maximum vibration level and the level directly above the excitation.

However, it is found that the shadow effect can also be present even without the existence of the tunnel structure. Therefore, the characteristics of the shadow effect will be studied with an analytical ground model in the next section before investigating the effects of the tunnel structure in subsequent sections.

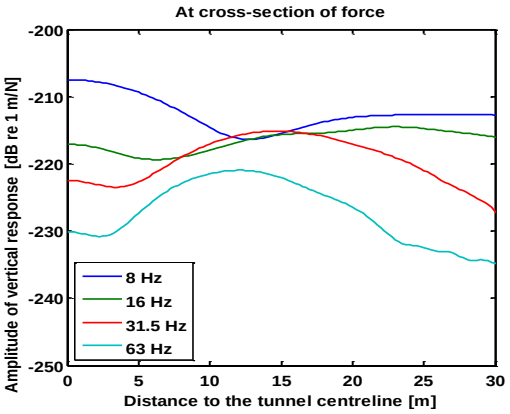

Figure 2. Vertical response on the ground surface at different frequencies to a unit force at the tunnel base.

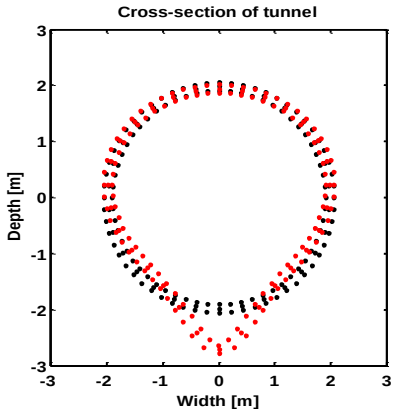

Figure 3. Displacement of tunnel structure for a force at the base at 31.5 Hz.

4. The characteristics of the shadow effect

An analytical ground model, based on Kausel and Roësset [9], is used here to study the shadow effect on the ground surface due to the excitation at a certain depth. In this model, the ground is represented by the stiffness matrices of various layers expressed in the wavenumber domain. The model is considered to be axisymmetric. To allow the introduction of a force, an interface between two soil layers is introduced at the location of the force. However, the soil properties beneath and above the interface are kept the same in order to model the ground as a homogeneous half-space. The force is applied over a circular area of diameter 0.6 m (The size of the force area has no effect to the size of shadow area). The displacements at the ground surface are monitored at a spacing of 0.5 m. Results are presented for different ground properties. The soil properties used in the ground model are initially based on typical London clay, as shown in table 1. Based on these properties, other artificial soils are considered by varying the values of compressional or shear wave speed.

The pseudo-resultant responses ($\sqrt{|u_y|^2 + |u_z|^2}$, with u_y and u_z the horizontal / vertical components of vibration) on the ground surface to the excitation on the ground (at 0 m) and in the ground (at 5, 10 and 15 m depth) are plotted in figure 4. The displacements at four different excitation frequencies are plotted against the lateral distance from the excitation force. For the excitation at the ground surface, the peak response occurs at the force location. For the excitation at various depths, the maximum response can be found at some distance away from the excitation point, at least at higher frequencies.

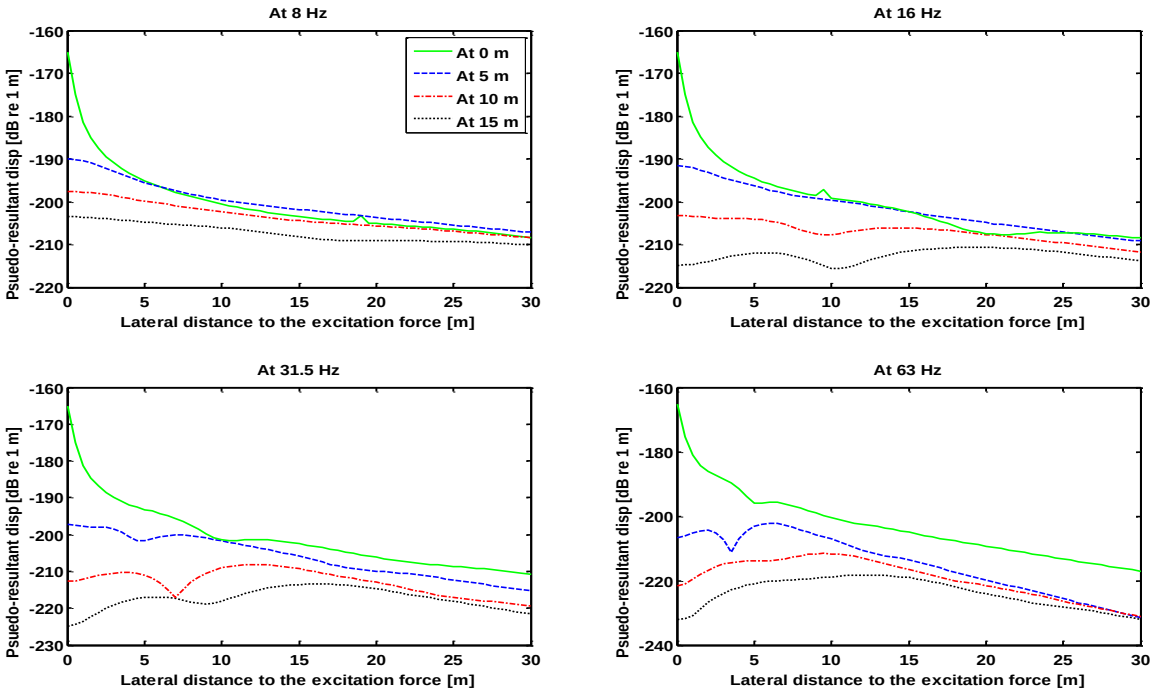

Figure 4. Displacements on the ground surface to the excitation at different frequencies and depths.

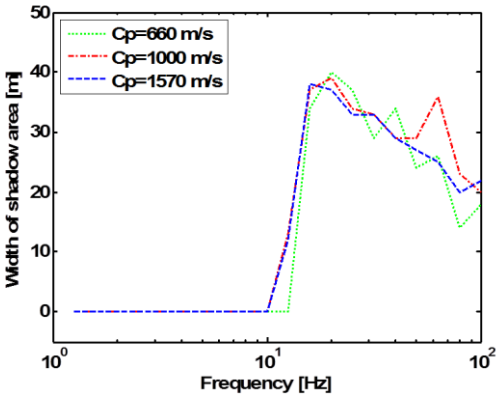

Figure 5. Width of shadow area plotted against frequency for different soil P-wave speeds; depth of force 15 m.

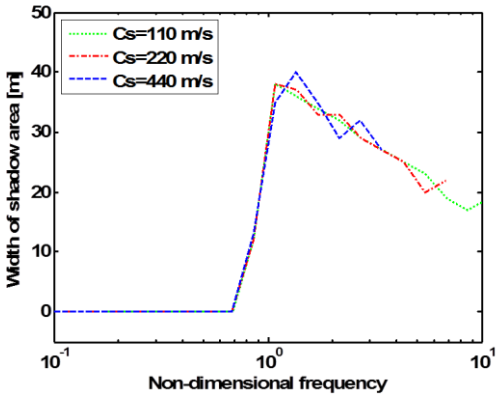

Figure 6. Width of shadow area plotted against non-dimensional frequency fd/c_s for different soil S-wave speeds; depth of force 15 m.

Three cases are calculated next to examine the response on the ground surface to a vertical excitation at 15 m below the ground surface. Three values of P-wave speed are used for the soil, which are 1570 (as used previously), 1000 and 660 m/s while the S-wave speed is kept as 220 m/s. (Poisson's

ratio: 0.49, 0.44 and 0.33). When the width of the shadow area (as defined in Section 3) is displayed against the frequency in figure 5, it can be seen that the width is only slightly influenced by the compressional wave speed in the ground. A distinct cut-on frequency can be seen at 10 Hz, above which the maximum response occurs at some distance away from the excitation point and this distance decreases with the increase of excitation frequency.

Varying the shear wave speed there is a clear change in the cut on frequency; for a lower value of shear wave speed the cut on frequency reduces. This is shown in figure 6 by plotting the width of the shadow zone against a non-dimensional frequency fd/c_s, where f is the frequency, d is the depth and c_s is the shear wave speed. This corresponds to the ratio of the depth to the shear wavelength in the soil. As well as London clay considered above, for which the shear wave speed is 220 m/s, results are shown for two artificial grounds in which the shear wave speed is halved or doubled, while the P-wave speed is 1570 m/s, the same as the London clay. As shown in figure 6, the cut-on occurs at a non-dimensional frequency of unity in each case.

Figure 7 compares the width of the shadow area on the ground surface for excitation at three different depths. The widths of the shadow area are shown normalised by the excitation depths in each case. The cut-on frequency is found to be inversely proportional to the depth, giving a constant value of non-dimensional frequency. The ratio of the width of the shadow area to the excitation depth is the same in each case. This means the deeper the excitation, the wider the shadow effect area is. Above the cut-on frequency, the shadow area gradually becomes smaller at higher frequencies.

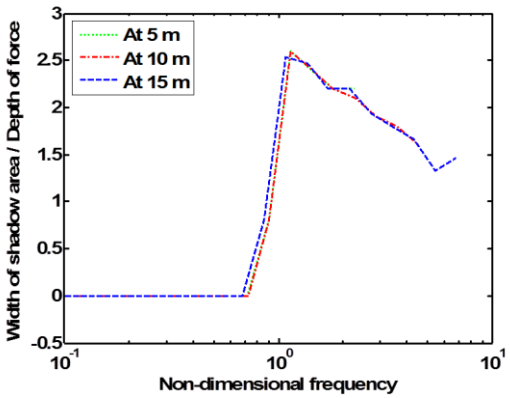

Figure 7. Width of shadow area plotted against non-dimensional frequency fd/c_s compared for force at different depths.

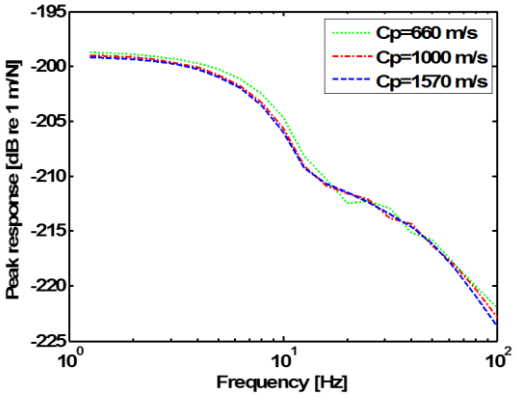

Figure 8. Maximum response plotted against frequency for different soil P-wave speeds; depth of force 15 m.

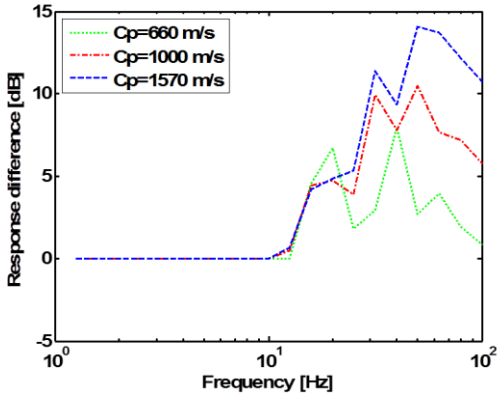

Figure 9. Response level difference plotted against frequency for different soil P-wave speeds; depth of force 15 m.

The maximum responses of the cases with different compressional wave speeds are shown in figure 8 against frequency; thus at each frequency above the cut-on the response plotted corresponds to a different lateral position. The level difference between this maximum response and the response directly above the force is shown in figure 9. It can be seen in figure 8 and figure 9 that the P-wave speed in the soil has less influence on the amplitude of the maximum response on the ground surface, but it influences the response level difference above 10 Hz where the vibration level above the tunnel structure is smaller. From figure 9, it can also be seen that the shadow area grows deeper with the decrease of P-wave speed in the soil.

Similarly, the maximum responses and the response level difference of the cases with different shear wave speeds are shown in figure 10 and figure 11. The maximum response on the ground surface is higher with the decrease of S-wave speed in the soil, as shown in figure 10. The shadow area is also deeper for the case with lower S-wave speed, as shown in figure 11. Moreover, as shown in figure 6, it can be seen that the cut-on frequency increases with the S-wave speed.

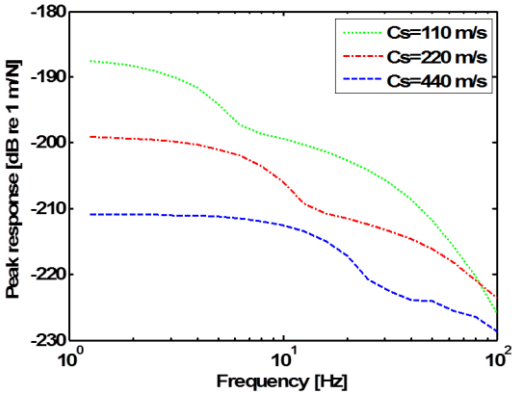

Figure 10. Maximum response plotted against frequency for different soil S-wave speeds; depth of force 15 m.

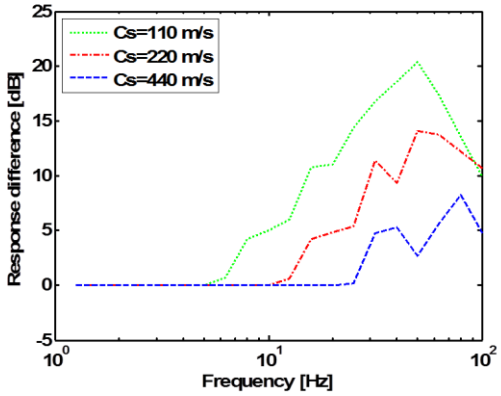

Figure 11. Response level difference plotted against frequency for different soil S-wave speeds; depth of force 15 m.

5. With the existence of lined and unlined tunnel

It has been seen, from the comparison of figure 2 and figure 4, that the vibration induced by a force acting on the tunnel base is similar to that obtained by the ground model excited by the force at the depth of railhead position. In this section the results with and without the tunnel structure are compared.

To study the shadow effect in the ground with the existence of a lined tunnel, the WANDS model described in Section 2 is used to calculate the responses on the ground surface to the excitation at the tunnel bottom. To consider an unlined tunnel, the material of the tunnel in the model is replaced with that of the surrounding soil. The depth is 15 m from the ground surface to the tunnel centreline, 16.905 m to the force point. For the ground model without tunnel, the force is applied at the same depth as that in the tunnel-ground model.

Figure 12 compares the pseudo-resultant vibration on the ground surface due to a unit force. Three models are compared: the analytical model in which the force is applied in the soil, a WANDS model including the tunnel structure and one with an unlined tunnel cavity. At 8 Hz, the responses on the ground surface are the largest for the case without the tunnel. As the frequency increases, the responses from the tunnel-ground model gradually increase relative to the ground model and they exceed that from the ground model at some distances. It can be clearly seen that the maximum response is enlarged due to the presence of tunnel but the shadow area is reduced in width. This is confirmed in figure 13 which shows the widths of the shadow area in the three cases, plotted against frequency. This is because, with the existence of the tunnel, the vibration above the structure depends

on the excitation from the tunnel crown, rather than the tunnel bottom, which corresponds to a shallower force in the ground.

Comparing the results between the model with the lined tunnel and the model with the unlined tunnel, the difference is that the cut-on frequency of the model with unlined tunnel is slightly higher and the shadow area is slightly narrower.

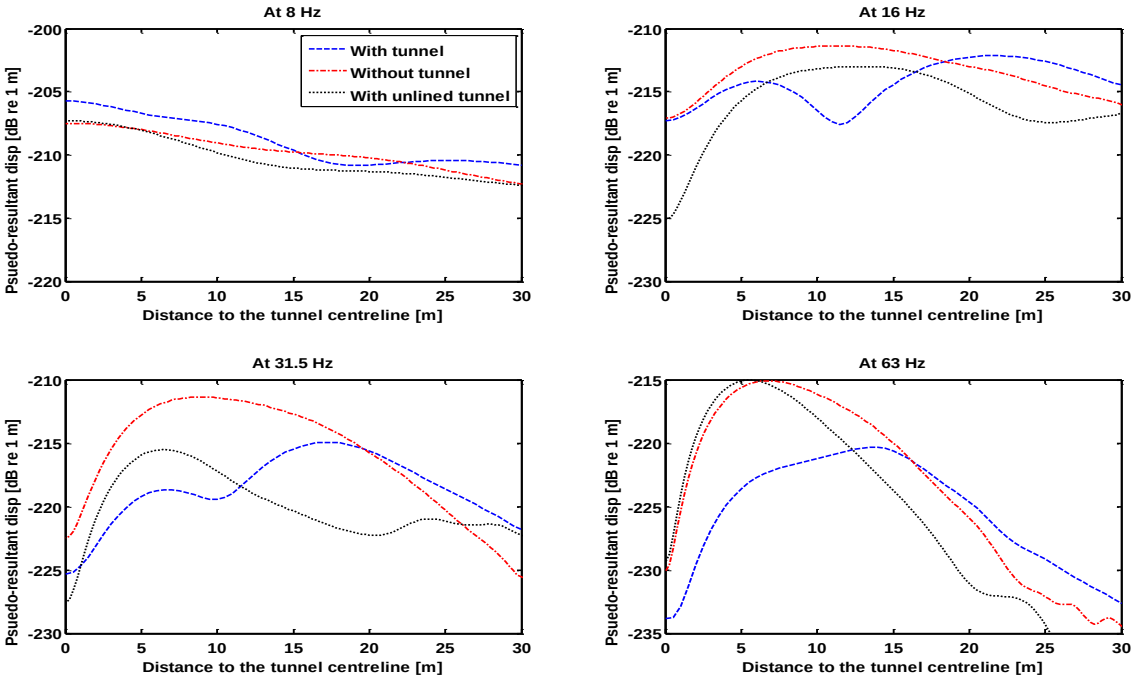

Figure 12. Pseudo-resultant responses to a unit force compared at four excitation frequencies for three different models.

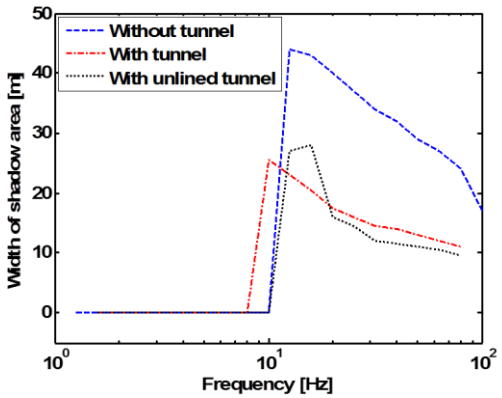

Figure 13. Width of shadow area plotted against frequency for three different models.

6. Influence of tunnel properties

As shown in the previous section, the characteristics of the shadow effect differ not only between the models with and without tunnel, but also differ slightly between the lined and unlined tunnel. In this section, the influence from the diameter and thickness of the tunnel lining on the shadow effect at the ground surface is studied.

The width of the shadow area is shown in figure 14 for two different tunnel diameters. The inner diameters of the tunnels are 3.81 and 5.675 m for the small and large tunnel respectively. For both

tunnels, the lining thickness is 220 mm and the tunnel depth is now 25 m from the ground surface to the tunnel centre. This shows that, although the cut-on frequency is slightly lower, the shadow area caused by the large tunnel is slightly narrower than that caused by the small tunnel, which is the opposite effect to what would be expected from a purely acoustical shadow. Similar to the conclusion in figure 13, the location of tunnel crown contributes more than the tunnel bottom to the shadow area above the structure. The crown of the small tunnel is about 1 m deeper than that of the large tunnel, which results in the shadow area of the small tunnel being slightly wider.

Figure 15 shows the influence of the lining thickness on the shadow area at the ground surface. All the tunnels have the same inner diameter which is 3.81 m, while the outer diameter is varying to give different lining thickness. It can been seen that the lining thickness has a rather small impact on the response at the ground surface, giving shadow areas that are quite similar for all frequencies.

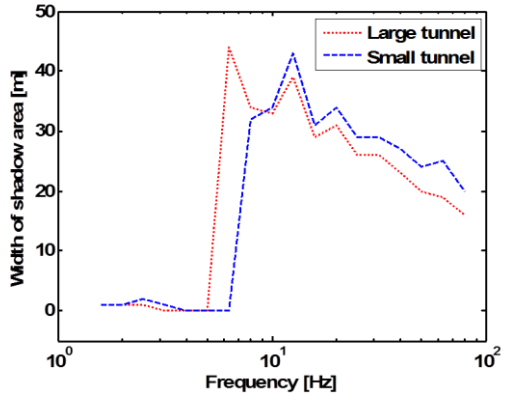

Figure 14. Width of shadow area plotted against frequency for different tunnel diameters. Depth of tunnel 25 m.

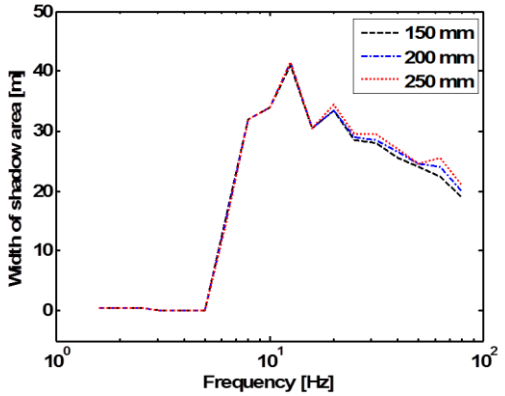

Figure 15. Width of shadow area plotted against frequency for different lining thicknesses. Depth of tunnel 25 m.

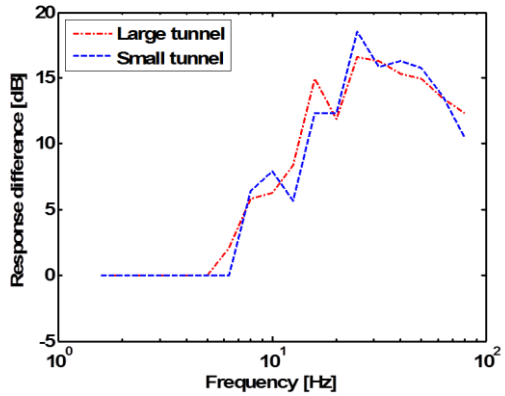

Figure 16. Response level difference plotted against frequency for different tunnel diameters. Depth of tunnel 25 m.

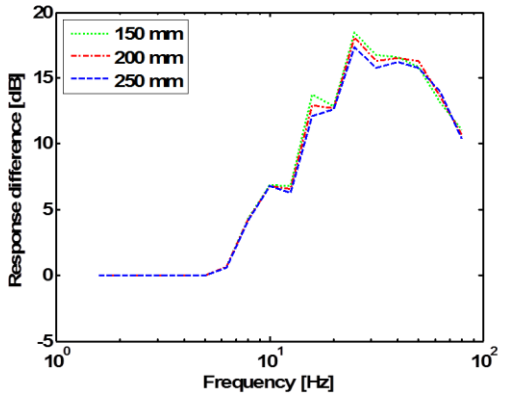

Figure 17. Response level difference plotted against frequency for different lining thicknesses. Depth of tunnel 25 m.

The ratio of the maximum response to the response at 0 m is plotted in figure 16 and figure 17 for the cases with different tunnel diameters and lining thickness. It can be seen that the size of the tunnel structure has little influence on the depth of the shadow area.

7. Conclusions

In this study of vibration at the ground surface from a tunnel using the 2.5D FE / BE model, it has been found that the maximum vibration occurs at some distance from the tunnel centreline for frequencies above a certain value. The vibration directly above the tunnel is up to 10 dB lower, like a

shadow effect. It has been found that this phenomenon also exists in a half-space without a tunnel when the force is applied at certain depth in the soil.

Three parameters have been defined to describe the characteristics of the shadow effect. The first is the cut-on frequency, above which the maximum response no longer occurs directly above the excitation force. The second is the width of the shadow area which is twice the distance from the maximum response to the projection of the force on the ground surface. The third parameter is the level difference between the maximum response and that directly above the force.

Using the analytical ground model, the influence of the soil properties and excitation depth on the cut-on frequency and size of shadow area has been studied. The cut-on frequency is found to be proportional to the shear wave speed and inversely proportional to the depth of the excitation force in the soil. Based on the results from the WANDS model, the influence due to the presence of the tunnel is also studied. It is found that the shadow area is narrower in the presence of a tunnel than without a tunnel. Moreover, for a larger tunnel ring, the shadow area is found to be narrower.

References

[1] Jones C, Thompson D and Petyt M, A model for ground vibration from railway tunnels, *Proceedings of the ICE-Transport* **153**.2 (2002) 121-129.

[2] He X, Cao Y and Zhang N. Numerical analysis of vibration effects of metro trains on surrounding environment. *International Journal of Structural Stability and Dynamics* **7**.01 (2007) 151-166.

[3] Hussein M, Hunt H, Rikse L, Gupta S, Degrande G, Talbot J, François S, Schevenels M. Using the PiP model for fast calculation of vibration from a railway tunnel in a multi-layered half-space. *Notes on Numerical Fluid Mechanics and Multidisciplinary Design,* **99***,* Springer (2008): 136-142.

[4] Andersen L and Jones C. Coupled boundary and finite element analysis of vibration from railway tunnels—a comparison of two-and three-dimensional models. *Journal of Sound and Vibration* **293**.3 (2006): 611-625.

[5] Lombaert G and Degrande G. Ground-borne vibration due to static and dynamic axle loads of InterCity and high-speed trains. *Journal of Sound and Vibration* **319**.3 (2009): 1036-1066.

[6] Sheng X, Jones C, Thompson D. Modelling ground vibration from railways using wavenumber finite-and boundary-element methods. *Proceedings of the Royal Society A: Mathematical, Physical and Engineering Science* **461**.2059 (2005) 2043-2070.

[7] Nilsson C and Jones C. Theory manual for WANDS 2.1, *ISVR technical memorandum* No.**975**. 2007, University of Southampton UK

[8] Degrande G, Clouteau D, Othman R, Maarten A, Hamid C, Ralf K, Pranesh C, and Bram J. A numerical model for ground-borne vibrations from underground railway traffic based on a periodic finite element–boundary element formulation. *Journal of Sound and Vibration* **293**.3 (2006) 645-666.

[9] Kausel E and Roësset J. Stiffness matrices for layered soils. *Bulletin of the Seismological Society of America* **71**.6 (1981): 1743-1761.